Lab on a Chip

Rapid imaging, detection, and quantification of *Nosema ceranae* spores in honey bees using mobile phone-based fluorescence microscopy

Journal:	*Lab on a Chip*
Manuscript ID	LC-ART-12-2018-001342.R1
Article Type:	Paper
Date Submitted by the Author:	23-Jan-2019
Complete List of Authors:	Snow, Jonathan; Barnard College, Biology Ceylan Koydemir, Hatice; UCLA, Electrical Engineering Dept. Karinca, Doruk; Univeristy of California Los Angeles , Computer Science Liangus, Kyle; University of California, Los Angeles , Computer Science Tseng, Derek; UCLA, EE Ozcan, Aydogan; UCLA, Elect. Eng.

Lab on a Chip

ARTICLE

Rapid imaging, detection, and quantification of *Nosema ceranae* spores in honey bees using mobile phone-based fluorescence microscopy

Received 00th January 20xx,
Accepted 00th January 20xx

DOI: 10.1039/x0xx00000x

www.rsc.org/

Jonathan W. Snow*[a], Hatice Ceylan Koydemir[b,c,d], Doruk Kerim Karinca[e], Kyle Liang[e], Derek Tseng[b], Aydogan Ozcan*[b,c,d]

Recent declines in honey bee colonies in the United States have put increased strain on agricultural pollination. *Nosema ceranae* and *Nosema apis,* are microsporidian parasites that are highly pathogenic to honey bees and have been implicated as a factor in honey bee losses. While traditional methods for quantifying *Nosema* infection have high sensitivity and specificity, there is no field-portable device for field measurements by beekeepers. Here we present a field-portable and cost-effective smartphone-based platform for detection and quantification of chitin-positive *Nosema* spores in honey bees. The handheld platform, weighing only 374 g, consists of a smartphone-based fluorescence microscope, a custom-developed smartphone application, and an easy to perform sample preparation protocol. We tested the performance of the platform using samples at different parasite concentrations and compared the method with manual microscopic counts and qPCR quantification. We demonstrated that this device provides results that are comparable with other methods, having a limit of detection of $0.5x10^6$ spores per bee. Thus, the assay can easily identify infected colonies and provide accurate quantification of infection levels requiring treatment of infection, suggesting that this method is potentially adaptable for diagnosis of *Nosema* infection in the field by beekeepers. Coupled with treatment recommendations, this protocol and smartphone-based optical platform could improve the diagnosis and treatment of nosemosis in bees and provide a powerful proof-of-principle for the use of such mobile diagnostics as useful analytical tools for beekeepers in resource-limited settings.

Introduction

The western honey bee, *Apis mellifera,* provides pollination services of critical importance to humans in both agricultural and ecological settings[1]. Honey bee colonies have suffered from increased mortality in recent years caused by a complex set of interacting stresses. Nutritional stress due to loss of appropriate forage, chemical poisoning from pesticides, changes to normal living conditions brought about through large-scale beekeeping practices, and infection by pathogens are all implicated in this phenomenon[2].

The microsporidian species, i.e. *Nosema ceranae* and *Nosema apis,* cause individual mortality in honey bees and may contribute to the death of diseased colonies[3-5]. Obligate intracellular parasites, these unicellular eukaryotes infect the midgut of honey bees and cause significant pathology at the individual and colony levels. *N. apis* has been recognized as an important pathogen of honey bees for over a 100 years[6]. *N. ceranae* was first identified in the late 1990's in the Asian honey bee (*Apis cerana*)[7], has quickly become highly prevalent in managed colonies of European honey bees all over the world[8,9], and has been observed in other hymenopteran species as well [10-14].

N. ceranae spores infect the midgut of honey bees, causing energetic stress, epithelial damage, and when untreated, death. In addition, infection has been associated with a number of physiological and behavioral changes that likely affect individual contribution to a colony (reviewed in Ref.5). *N. ceranae* infection can currently be controlled by treatment with the drug Fumagillin (reviewed in Ref.15), a methionine aminopeptidase-2 inhibitor. However, high doses of this drug are toxic to all eukaryotic cells and evidence suggests that *N. ceranae* can evade suppression in some circumstances[16], suggesting the need for alternative treatment strategies. In addition, no easy, cost-effective, and reliable field test for

[a] *Department of Biology, Barnard College, New York, NY, 10027, USA;*
[b] *Electrical and Computer Engineering Department, University of California at Los Angeles, Los Angeles, CA, 90095, USA*
[c] *Bioengineering Department, University of California at Los Angeles, Los Angeles, CA, 90095, USA*
[d] *California NanoSystems Institute (CNSI), University of California at Los Angeles, Los Angeles, CA, 90095, USA*
[e] *Computer Science Department, University of California at Los Angeles, Los Angeles, CA, 90095, USA*
** To whom correspondence should be addressed:*
Department of Biology, Barnard College, New York, NY 10027, USA
Phone: 212-854-2084 fax: 212-854-1950, Email: jsnow@barnard.edu; OR
UCLA Electrical and Computer Engineering Department, Los Angeles, CA 90095; Phone: 310-825-0915; E-mail: ozcan@ucla.edu
Electronic Supplementary Information (ESI) available. See DOI: 10.1039/x0xx00000x

Nosema infection exists, causing Fumagillin to be administered regardless of the presence or absence of infection. This overuse likely causes sub-lethal health issues in treated colonies, reduces flexibility of honey production for human consumption, and could lead to resistance to the drug if continued[17].

Because diagnosis has been identified as *a major challenge* for the treatment of *Nosema* infection in honey bees[15], a cost-effective field detection method would be highly valuable. Previous methods for quantifying *Nosema* infection[18] include manual spore counting using light microscopy[19], quantitative PCR[20], enzyme-linked immunosorbent assay (ELISA)[21], *in situ* hybridization[22], and through the use of DNA dyes[23,24]. While all these methods have important advantages, development of additional methods with potential for use in the field is warranted.

We previously showed that the chitin-binding agent Fluorescent Brightener 28 (FB28) (Calcifluor White M2R) could be used to detect *N. ceranae* in individual experimentally infected bees and individual bees from infected colonies[25]. Here we describe a field-portable and cost-effective smartphone-based fluorescence microscope and a custom-designed application for the rapid imaging, detection, and quantification of *Nosema* spores in honey bees (Fig. 1).

This field-portable and cost-effective microscope weighs only 374 g (including the smartphone) and uses three AA batteries to power four ultraviolet (UV) light emitting diodes (LEDs) used as excitation light source. The microscope has an external lens for magnification of the sample image and is equipped with an emission filter for the detection of fluorescently tagged parasite spores. For a given sample of interest, honey bee tissue is homogenized, fluorescently labeled, and prepared for image capture on a standard microscope slide with a coverslip, which is placed on a slide-holder attachment of the portable microscope for fluorescence imaging (Fig. 2).

We also custom-developed a smartphone application[26] that can process raw format images, acquired using the smartphone based microscope, transmitted to our servers. After starting the application and turning on the LEDs, an image is captured and sent to our servers for automated detection and counting of spores on the image using our custom developed image processing algorithms. In less than two minutes, image processing is finished and the spore count result is sent back to the smartphone screen through the same application (Fig. 3).

We used *Nosema* spore suspensions at different concentrations to test the performance of the platform and the results demonstrated that infection levels quantified by this mobile optical platform correlate well with detection by two other methods; spore counts using light microscopy and qPCR.

Coupled with treatment recommendations, this protocol and device could improve the diagnosis and treatment of nosemosis in bees and provide a powerful proof-of-principle for the use of such mobile diagnostics technologies in agricultural settings.

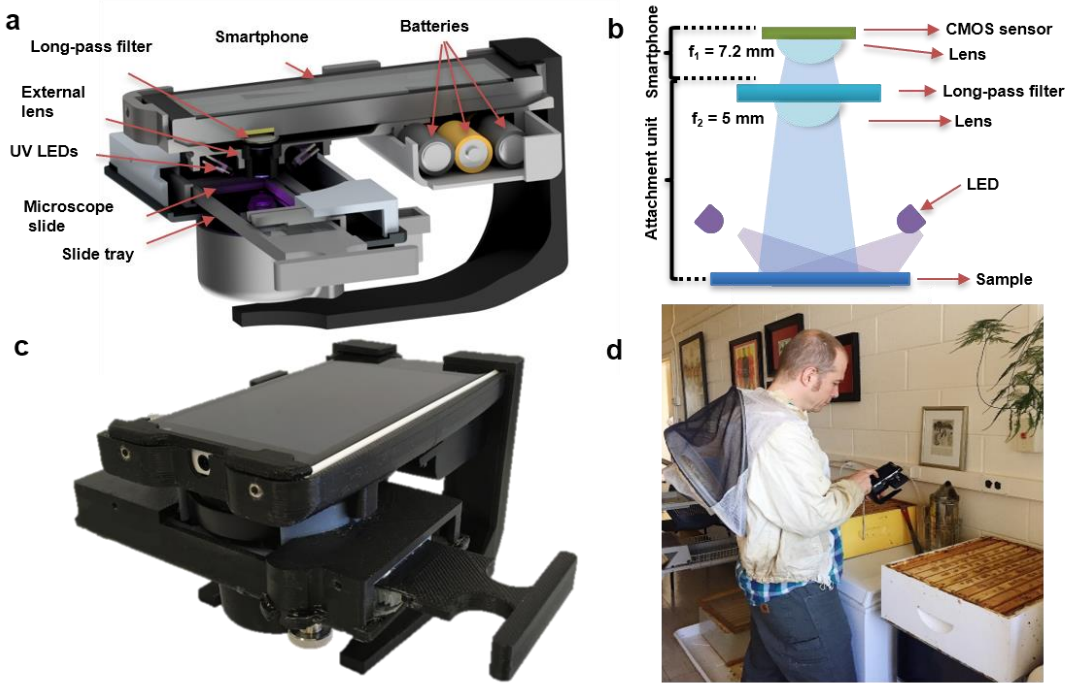

Fig. 1. Schematic illustrations of (a) the prototype and (b) illumination scheme. (c) A photo of the prototype. (d) A photo demonstrating the use of the portable smartphone-based platform.

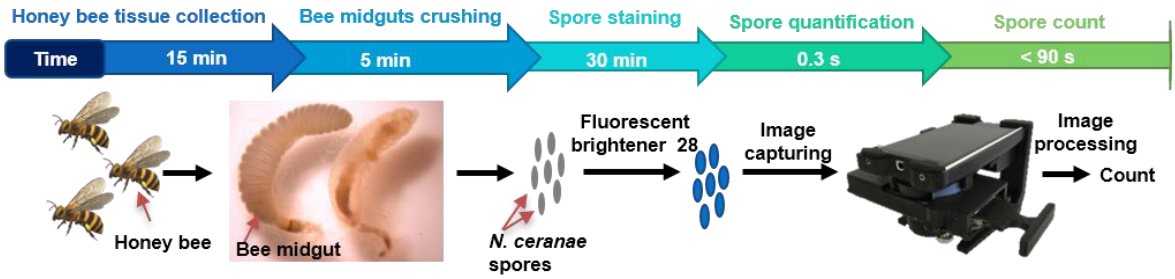

Fig.2. Sample preparation steps.

Materials and Methods

Honey bee tissue collection

Honey bees were collected from outbred colonies consisting of a typical mix of *Apis mellifera* subspecies found in North America at different times during the months of April-October from the Barnard College apiary (New York, NY, N 40.809974, W73.962904). Honey bees were collected from the landing board of sampled colonies and likely represent a mix of bees that is predominantly foragers. Only visibly healthy bees were collected and all source colonies were visually inspected for symptoms of common bacterial, fungal, and viral diseases of honey bees. Gut tissue was removed from abdomens and midguts were dissected. For colony level analysis the midguts from 12 bees per colony were pooled for further analysis.

Chitin staining

For chitin staining, midguts were crushed in 0.5 ml H_2O per bee using a dounce homogenizer. After bringing the composition to 1x PBS (137 mM NaCl, 2.7 mM KCl, 4.3 mM Na_2HPO_4, 1.47 mM KH_2PO_4, pH of 7.4.), the sample was incubated with 0.001% FB28 (also known as Calcifluor White M2R (Sigma, St Louis, MO)), for 30 min at room temperature (27° C). Visualization of FB28 bound spores was performed using NIKON Elipse E600FN (Nikon, Melville, NY). For Solophenyl Flavine 7GFE 500 (Direct Yellow 96, DY96) and Pontamine Fast Scarlet 4B (Direct Red 23, DR23) staining, the sample was incubated in PBS with 0.001% DY96 or 0.001% DR23, for 30 min at room temperature (27° C). Visualization of spores was performed using NIKON Elipse E600FN (Nikon, Melville, NY).

Design of the smartphone-based microscope

We used Nokia Lumia 1020 as our smartphone in the design of the microscope; the rear camera of the smartphone has 41 MP and provides raw format images (i.e. digital negative (DNG)) as well as JPG. A compact lens, f = 7.2 mm is embedded on the camera module of the smartphone and the complementary metal–oxide–semiconductor (CMOS) image sensor has 1.12 µm pixel size. Exposure time, white balance, ISO, and auto-focus can be adjusted using the regular camera application of the smartphone. We used 0.5 s as exposure time, 100 as ISO value, and daylight as white balance throughout the experiments to capture fluorescence images of the spores on glass cover slips.

Our smartphone-based fluorescence microscope uses an external lens with a focal length of f = 5 mm (product no. LS-40166, eBay) for magnification and has a sub-micron spatial resolution (see Fig. 1). It uses four UV LEDs (product no. VLMU3500-385-060CT-ND, Digi-key Inc.) as excitation light source, which are powered using three AA batteries. Emission from FB 28 labelled *Nosema* spores is filtered through an emission filter (product no. ET460/50m, Chroma Technology Corp.) and detected using the image sensor of the rear camera of the smartphone. The opto-mechanical attachment unit is designed using Autodesk Inventor Professional software and printed using a 3D printer (Stratasys Ltd.). The unit has a sample tray that allows user to analyze a microscope slide over a large field of view (i.e., ~15 mm x ~35 mm) by manually scanning the slide in x and y directions. This portable microscope has also a z-stage for manual adjustment of the focal plane and auto-focusing on the sample can be achieved using the regular application of the smartphone. We coated interior surfaces of the attachment unit with black aluminum foil (product no. T205-1.0-AT205, Thorlabs Inc.) to reduce autofluorescence of the printed material under UV excitation.

Smartphone application for bee parasite spore detection

A Windows based smartphone application was developed for ease use of the platform and process images over a server. This smartphone application allows a user to capture a new image or select an existing image from a photo library and upload it to our servers for image processing using a custom developed image processing algorithm. The spore count result is sent back to the smartphone with the detailed information on location of the device and the date/time of the image captured through the application (Fig. 3).

The raw format image (.DNG) of the sample is captured and sent to our servers using the application. The image is converted to .TIFF file and blue channel of the image is extracted. After thresholding the image, it is converted to a binary image and the connected components with a pixel area of <60 are determined. These connected components detected on the 2D binary image are then automatically labelled and counted.

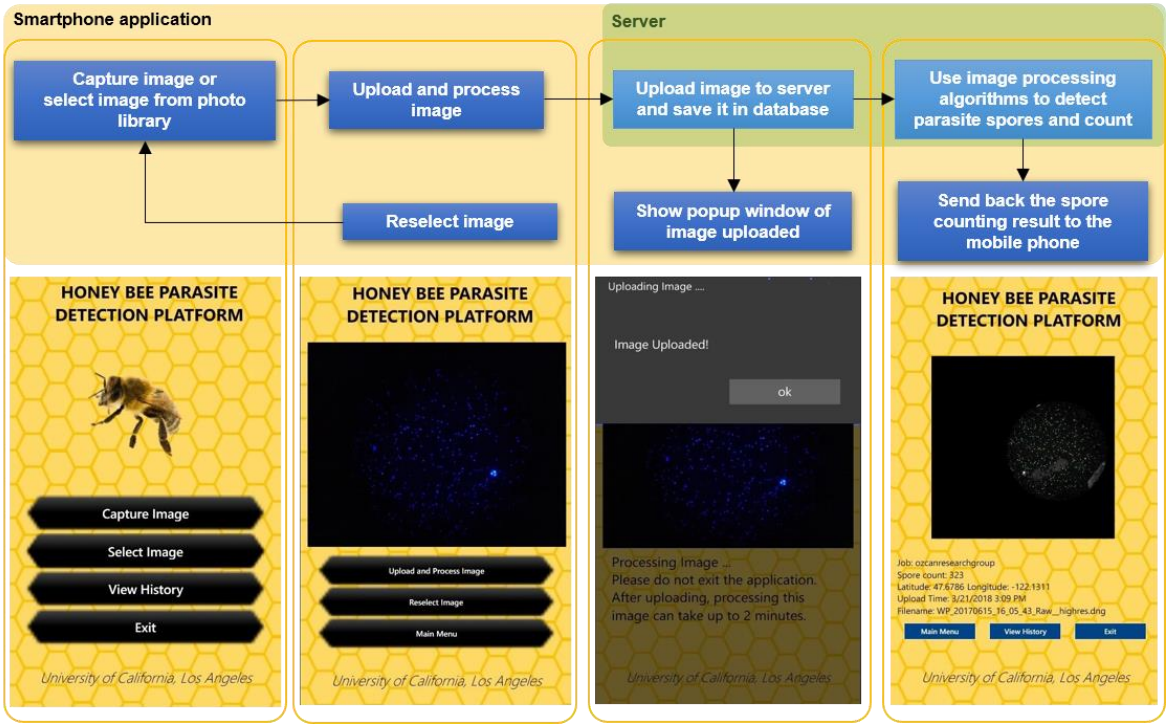

Fig. 3. Flow chart of the smartphone application for imaging, detection, and counting of *Nosema* spores using a smartphone-based microscope.

DNA Extraction and qPCR

DNA extraction was performed using a modified Smash & Grab DNA Miniprep protocol[27]. Subsequently, 1 µl of DNA was used as a template for quantitative PCR to determine the levels infection for *Nosema* sp. using the iQ SYBR Green Supermix (Biorad, Hercules, CA) in a LightCycler 480 thermal-cycler (Roche, Branchburg, NJ). Primer sequences for the 16S genes of *N. apis* were from the following study [13]. Primer sequences for *N. ceranae* genes *β-actin* (F: 5'- TCTGGTGATGGTGTCTCCCA-3', R: 5'-TGCCCATCAGGCATTTCGTA-3') and honey bee *ATP synthase F1 subunit alpha (ATP5a)* gene (F: 5'-TCCTTACGTTTGGTTTCTTCG-3', R: 5'-GGATCCGTATGATTATTGCAAAG-3') were developed for this study. The difference between the threshold cycle (Ct) number for honey bee *ATP5a* and that of the gene of interest was used to calculate the level infection relative to *ATP5a* using the $\Delta\Delta C_T$ method. A sample was considered negative for a specific *Nosema* species if it did not amplify any product by 35 cycles and zero was entered as the value in these cases.

Results and Discussion

To determine whether chitin-binding agents could be used to measure *N. ceranae* levels in naturally infected honey bees, we collected honey bees from an infected colony (qPCR revealed that this colony was negative for *N. apis* (data not shown)). First, we quantified the number of spores per bee using light microscopy ("light" panel in Fig. 4a). Then, we used the chitin-binding agent, FB28 to quantify the number of chitin-positive spores in the sample using fluorescence microscopy ("FB28"panel in Fig. 4a). When we plotted the spore count versus the FB28-positive cell count, we found a strong correlation between the two measurements (r^2=0.97, p<0.0001) (Fig. 4b). Even without any washing steps, the dye allowed for easy identification and counting of fluorescent structures resembling *Nosema* spores (Fig. 4c), which are distinctly oval structures of approximately 3.9-5.3 µm in length and 2.0-2.5 µm in width. We do observe other fluorescent structures, such as pollen grains and peritrophic matrix fragments, but these structures are easily distinguished from *Nosema* spores. No signal was observed in the absence of dye (Fig. S1).

In addition to the FB28 reagent, there are many available chitin-binding reagents with different light excitation and emission properties. Solophenyl Flavine 7GFE 500 (Direct Yellow 96, DY96)[28] and Pontamine Fast Scarlet 4B (Direct Red 23, DR23) that have been shown to stain chitin in fungal cell walls[29]. As these have different light excitation and emission properties than FB28, their performance was assessed for staining *Nosema* spores. DY96 also stained *Nosema* spores with similar properties as FB28, revealing spore-like structures in infected bees using the green filter (Fig. S1), while DR23 did not (data not shown). Pollen grains sometimes show autofluorescence signal in the green channel (unpublished observations). Thus, the FB28 reagent would be more useful than DY96 for distinguishing infection from high pollen content in the midgut lumen.

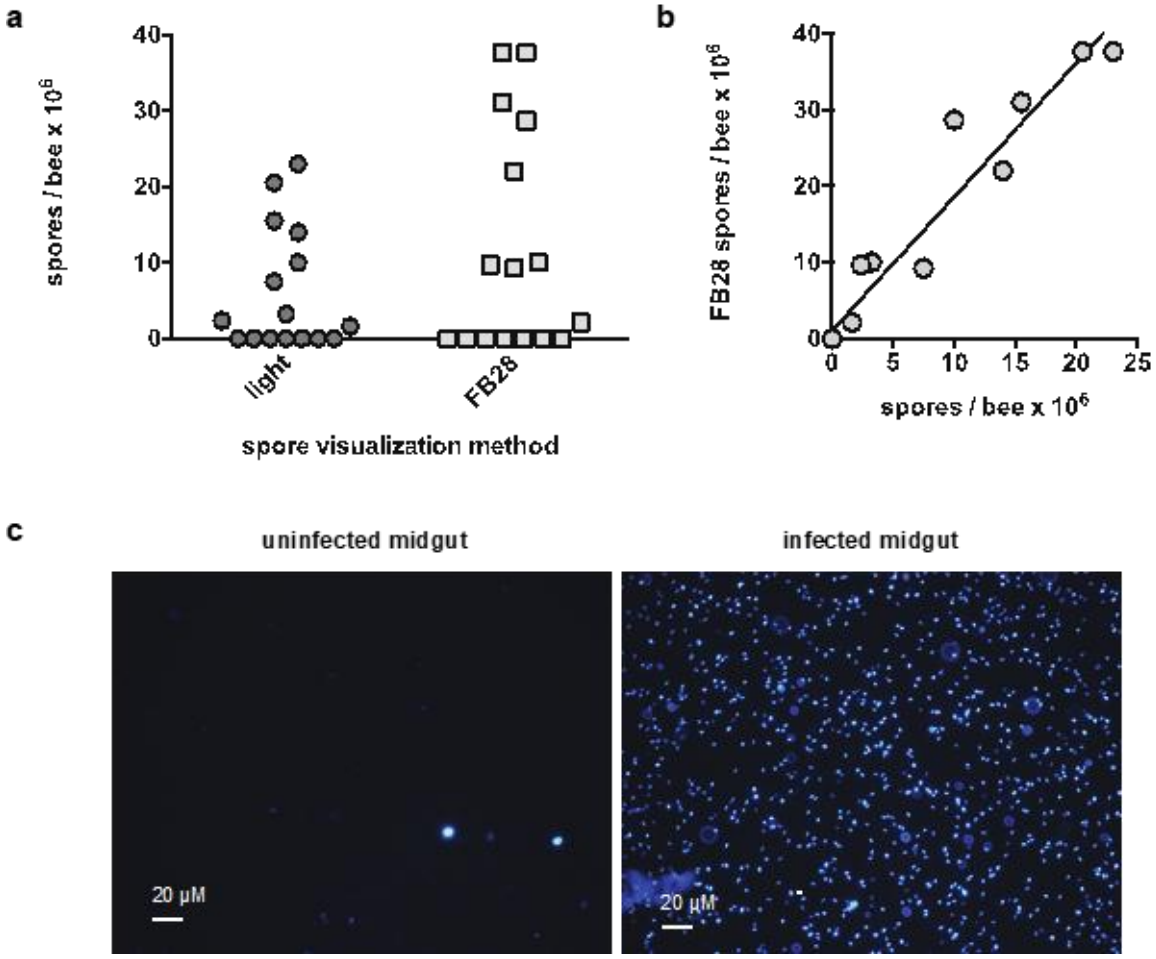

Fig. 4. Chitin-binding dye FB28 allows visualization of *Nosema ceranae* spores. *N. ceranae* levels as determined by spore count using light microscopy and by staining with FB28 in individual bees from a naturally infected colony (a). Correlation between spore counts using light microscopy and FB28 signal for individual bees from the infected colony (b). Midgut preparations from an uninfected and an infected bee (from an infected colony) with or without FB28 were visualized under UV excitation, using a 4x objective (c).

We tested the performance of the smartphone-based microscope (Fig. 1) in comparison to a benchtop microscope by imaging *Nosema* spore samples prepared according to the procedure described in Chitin staining subsection of Methods (Fig. 2). Fig. 5a shows the full field of view (FOV) image (~0.25 mm^2) captured using the mobile microscope. Approximately nine images using a 40 × objective lens need to be captured to cover the same field of view. Fig. 5b shows a zoomed-in image of a region on Fig. 5a. Each blue dot shown on Fig. 5b corresponds to a FB28 labelled *Nosema* spore. Fig. 5c-i and 5c-ii show the images obtained using a 20 × objective lens and the mobile-phone microscope, respectively. As shown in these figures, the image captured using the mobile-phone microscope is in good agreement with the image captured using a benchtop microscope equipped with a DAPI filter set.

To determine how this method compared with qPCR, *N. ceranae* infection levels were determined in parallel by spore count using traditional light microscopy, the smartphone method, and qPCR using primer for the *N. ceranae 16S* gene (Fig. S2). Similar results were observed using all methods, suggesting that the smartphone-based method compares favorably to quantification using molecular techniques.

We determined the limit of detection of the system and established the standard curve using the parasite spore suspensions at different concentrations. Seven samples were prepared from each suspension to capture images of the samples using the smartphone-based microscope. Also, four counts were performed using a light microscope by an expert (Fig. 6). The acquired images were then processed using a custom-developed image processing algorithm to detect the fluorescently labeled spores. The average of the automated count results from the mobile microscope was correlated with the average of the manual count results (using a benchtop microscope) for each concentration. The error bars were set to be positive and negative standard deviation of each measurement result. Therefore, horizontal error bars indicate the deviation in our manual counts, while vertical error bars are for the deviation coming from measurement results using

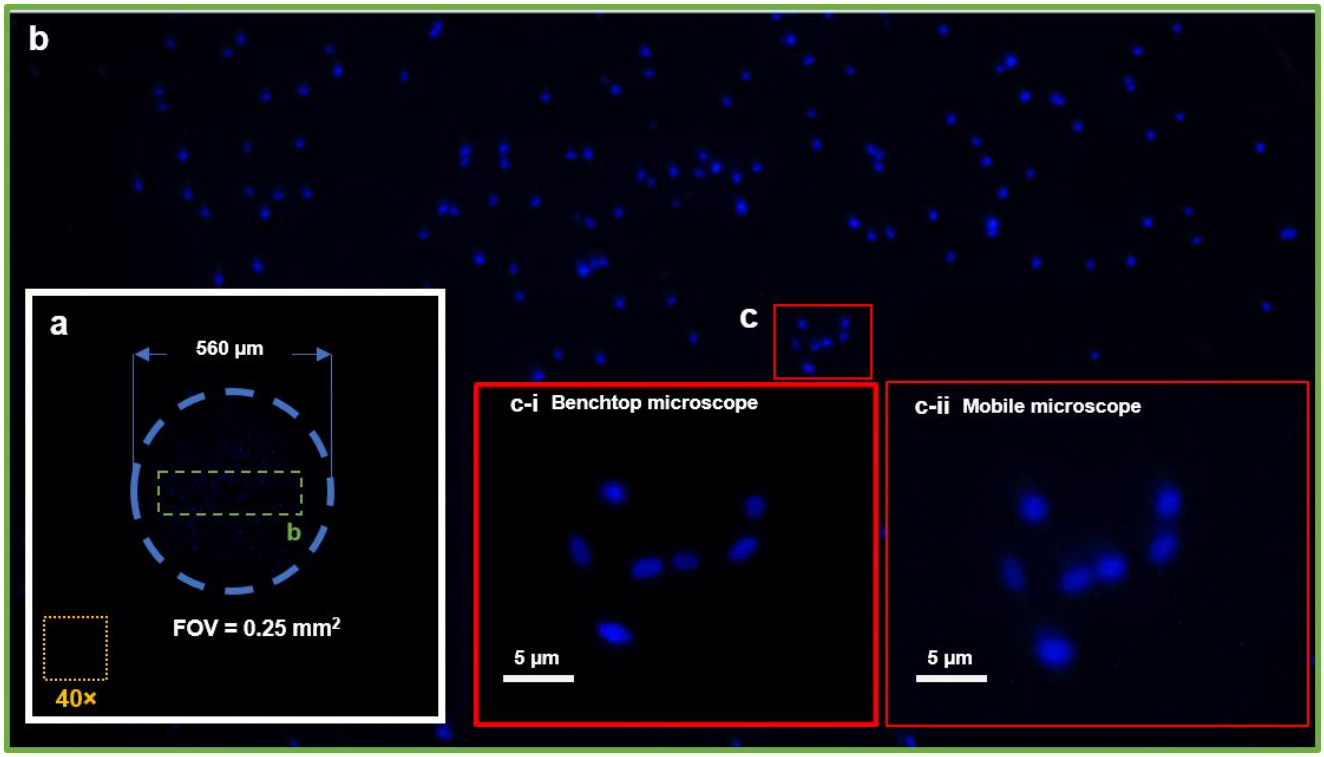

Fig. 5. Imaging performance of the smartphone-based microscope. (a) An image captured using the smartphone-based microscope, (b) A zoomed-in image of the green rectangle shown in (a). (c) A specific region showing fluorescently labelled Nosema spores on the smartphone-based image. (c-i) an image captured using a benchtop microscope (Olympus, 20 × objective lens, NA = 0.75) for comparison against the image captured using the mobile microscope (c). (c-ii) Zoomed in version of (c).

the portable device. The standard equation of the device was calculated by fitting a polynomial equation to the measurement points, i.e., $y = 2.413x^2 + 6.7385x + 3.875$, $R^2 = 0.99$. The limit of detection is calculated as 0.5×10^6 spores per bee, based on the mean cyst count for the control samples plus 3 times their standard deviation[26] (Fig. 6a and 6b).

We further blindly tested the performance of our mobile-phone based device using field samples and compared the results against the results obtained from a benchtop light microscope. Samples for the field test were obtained from colonies at the Barnard College apiary (New York, NY, N 40.809974, W73.962904) at 10 AM on 05/25/2018 and 05/29/2018 (Fig. 6c and 6d). As seen from Fig. 6c, the results obtained from the mobile phone microscope are good proxies of results obtained from our benchtop light microscope, at low to moderate concentrations. The relation between the results of our field-portable device and the benchtop microscope deviates about 30% at high spore concentrations. However, this deviation at high concentrations is not important since it is far beyond the spore concentration limit (i.e. 1×10^6 spores per bee) that is used to treat honey bees with a recommended concentration of fumagillin.

We also analyzed our technique against a benchtop light microscope using a Bland-Altman plot (Fig. 7). This plot shows a mean of -0.84×10^6 spores per bee, with the limits of agreement of 2.8×10^6 spores per bee and -4.5×10^6 spores per bee). There is only one outlier in Fig. 7, which is for a very high spore concentration. Our results indicate that this field-portable device together with the custom-developed smartphone application provides comparable results to manual spore counting using a benchtop microscope.

For the purposes of honey bee colony management, the use of chitin-biding reagents provides comparable data to spore counting and may offer an option to replace this technique for simple assessment of infection intensity in honey bee colonies in the field. Currently, the most commonly used methods are spore counting or methods that are unreliable, such as midgut morphology or presence of bee fecal matter on hive bodies[30]. When performed using a microscope of certain specifications, spore counting can be quite accurate. While the costs of microscopes with appropriate magnification have dropped in recent years, the use of a microscope with phase contrast capabilities, still prohibitively expensive, is recommended to prevent misidentification of other microbes and cellular debris as *Nosema* spores. Misdiagnosis and inaccurate determination of infection intensity can lead to implementation of inappropriate management decisions. Work is ongoing to define the sampling strategy that provides the most robust picture of prevalence and intensity of *Nosema* infection[15,31] as well as the

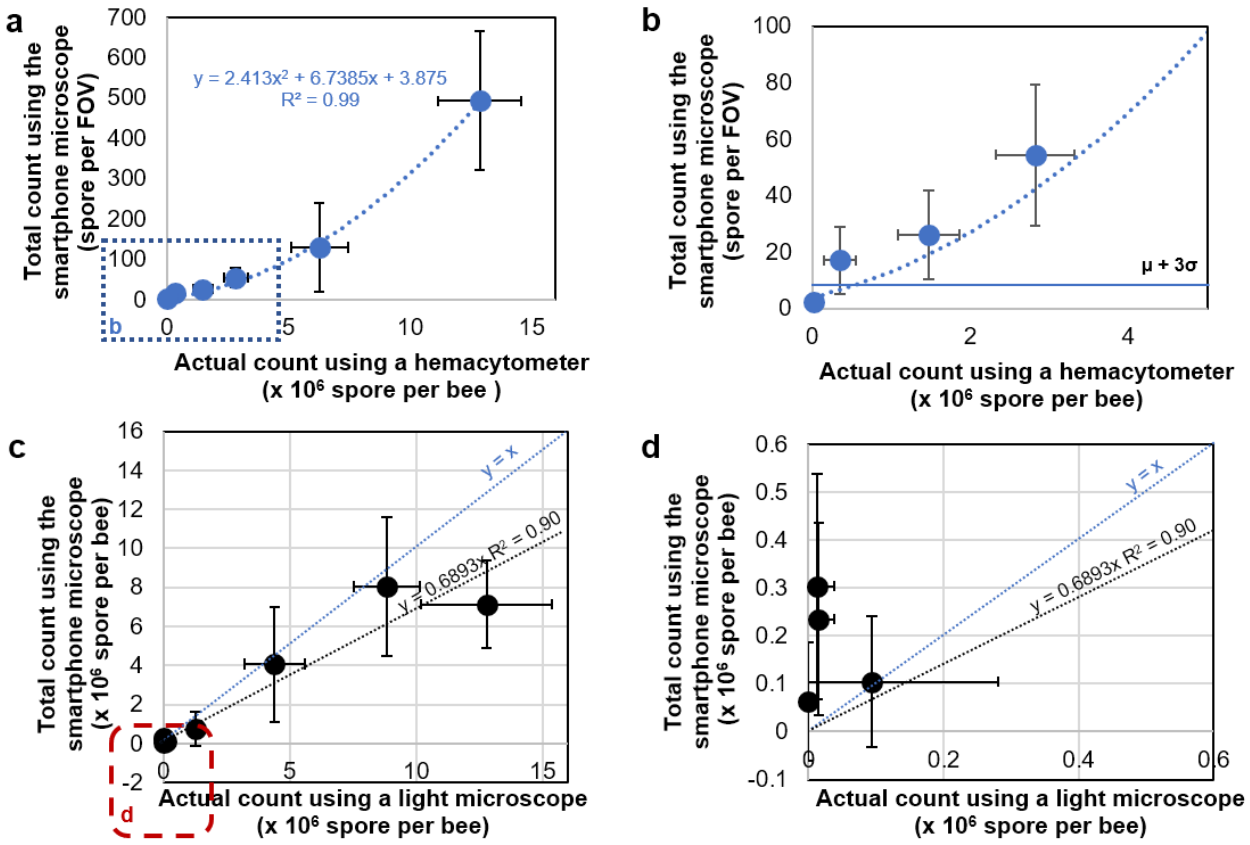

Fig. 6. Calibration curve and blind testing results for solutions containing various concentrations of *Nosema* spores. Each concentration is measured seven times using our smartphone-based microscope and four times using a benchtop light microscope. Error bars are equal to ± standard deviations of each measurement. (a) Calibration curve for our smartphone-based microscope. (b) Zoomed in version of (a), showing the total spore count per FOV using the smartphone microscope for a range of 0-100 x 10^6 per bee. (c) Estimated spore counts for various concentrations of *Nosema* spores against the concentration values obtained using a benchtop microscope. (d) Zoomed in version of (c).

best prediction of effects on the health of the colony. For example, the prevalence of infected bees is thought to be a more accurate indicator of infection intensity than the number of spores per bee measured for a pooled sample. In addition, spore loads alone may not be sufficient to determine the severity of *N. ceranae* infection and its impact on the health of a colony[32,33]. The age and location of sampled bees affect prevalence and intensity of infection[34-37]. Time of day, sampling size, and sampling frequency also all play a role[31]. Sampling of foragers maximizes sensitivity of detection as infection is typically spread between colonies by older individuals and spore loads increase with age[15]. Sampling of other age cohorts may provide additional information about the severity of infection at the colony level, specifically by providing information about whether infection has spread beyond the forager compartment. However, current recommendations for beekeepers advise that foragers are the most appropriate bees to sample [15].

In parallel, treatment guidelines based on the available diagnostic tools are also incomplete. Current recommendations advise treatment with the MetAP2 inhibitor, Fumagillin, if there are more than 1 million spores per bee in a pooled sample[15,30]. Furthermore, many investigators argue that infection by *Nosema* is not a threat to colonies and does not warrant treatment[15]. However, many beekeepers treat at seasonal intervals without testing for infection. Such antibiotic overuse can have multiple negative effects, including sub-lethal pathology in treated colonies, reduced flexibility of honey production for human consumption, and potential to induce resistance against the drug if continued. An easy and reliable monitoring method, such as that described here, could allow for more frequent assessment of infection and more timely management strategies.

Importantly, this assay should be easily adaptable for detection and quantification of other microsporidian parasites [38] of closely related insects, such as *Nosema bombi* in bumble bees[39] or other insects known to be infected with microsporidia[40,41]. In addition, as microsporidia infect diverse species that play important roles throughout the food production system[42], including fish, crustaceans, and other

beneficial insects, novel simple and inexpensive diagnostic methods would be expected to have broad implications.

This presented method also has some limitations. This assay does not allow distinguishing between microsporidian infections caused by the two *Nosema* species and should therefore be used in conjunction with other methods for determination of the *Nosema* species (*ceranae* or *apis*) if this is of interest to the users. In addition, meront, sporont, sporoblast, and immature spores are not detected by this method. However, these issues are also limitations of standard light microscopy. Using the knowledge of *N. ceranae* lifecycle, it may be possible to use the spore number or FB28 intensity to estimate the total pathogen load in infected bees. Finally, while this study demonstrates the feasibility of using smartphone-based fluorescence microscopy for the rapid imaging, detection, and quantification of *Nosema* spores in honey bees it is likely that improvements to the assay, equipment, and analysis could be made to improve usability and the graphical user interface.

In recent years, mobile diagnostic methods and devices have received increasing interest in biomedicine [43-47] and such strategies can likely be effectively employed in other resource limited situations, such as agricultural settings[48]. In fact, attempts to develop molecular diagnostics for identification of honey bee pathogens have been described[49] and one that is envisioned for use by beekeepers has been through limited tests in the field[50]. One avenue of research in the biomedical field has explored the use of microfluidic devices or microscopic devices coupled with smartphones for varied applications. For example, a device using LED, capillary-tube, and a modified ELISA assay coupled with a smartphone has been used to quantify *E. coli* levels in environmental samples[51]. Other have used optical imaging in conjunction with smartphones [52] to image viruses[53], as well as human pathogens , such as the blood fluke *Schistosoma haematobium*

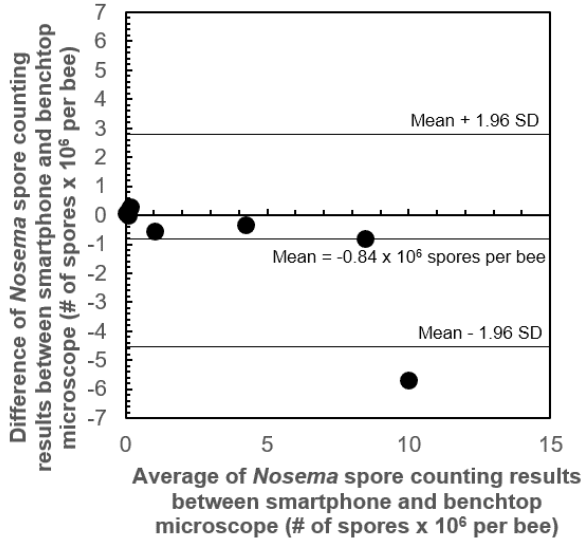

Fig. 7. The Bland‑Altman analysis, comparing the smartphone-based measurement results against the results of a benchtop microscope.

[54] and the protozoan *Giardia intestinalis*[26]. It seems likely that this assay could be developed further using similar strategies to produce a simplified and standardized assay that could provide an inexpensive and reliable means for assessing infection in honey bee colonies.

Conclusions

We presented a method coupling the chitin-binding dye FB28 with smartphone-based fluorescence microscope that allows for the rapid imaging, detection, and quantification of *Nosema* spores in honey bees. This technique could have a significant impact on the diagnosis and treatment of nosemosis in bees and other agriculturally important organisms and provide a powerful proof-of-principle for the use of such mobile diagnostics technologies in agricultural settings.

Author Contributions

J.W.S. and A.O. formulated the research goals and aims. J.W.S. performed all the experiments using bee parasite spores. H.C.K. and D.T. designed and tested the smartphone-based fluorescence microscope. H.C.K. developed the image processing algorithm and processed captured images using the mobile microscope. D.K. and K. L. developed the smartphone application. J.W.S., H.C.K. and A.O. wrote the manuscript. J.W. S. and A.O. supervised the research.

Acknowledgements

J.W.S. thanks the North American Pollinator Protection Campaign for their generous support in completion of this project. The authors acknowledge the technical assistance of Oluwajoba Akinyemi and Nina Deoras in the completion of select experiments. Ozcan Lab at UCLA acknowledges the support of NSF ERC and HHMI.

Notes and references

1 S. G. Potts, V. Imperatriz-Fonseca, H. T. Ngo, M. A. Aizen, J. C. Biesmeijer, T. D. Breeze, L. V. Dicks, L. A. Garibaldi, R. Hill, J. Settele and A. J. Vanbergen, *Nature*, 2016, **540**, 220–229.

2 D. Goulson, E. Nicholls, C. Botías and E. L. Rotheray, *Science*, 2015, **347**, 1255957.

3 I. Fries, *J Invertebr Pathol*, 2010, **103 Suppl 1**, S73–9.

4 R. Martín-Hernández, C. Bartolomé, N. Chejanovsky, Y. Le Conte, A. Dalmon, C. Dussaubat, P. García-Palencia, A. Meana, M. A. Pinto, V. Soroker and M. Higes, *Environmental Microbiology*, 2018, **20**, 1302–1329.

5 M. Goblirsch, *Apidologie*, 2017, **49**, 131–150.

6 I. Fries, *Bee World*, 1993, **74**, 5–19.

7 I. Fries, F. Feng, A. daSilva, S. B. Slemenda and N. J. Pieniazek, *European Journal of Protistology*, 1996, **32**, 356–365.

8 D. L. Cox-Foster, S. Conlan, E. C. Holmes, G. Palacios, J. D. Evans, N. A. Moran, P.-L. Quan, T. Briese, M. Hornig, D. M. Geiser, V. Martinson, D. vanEnglesdorp, A. L. Kalkstein, A. Drysdale, J. Hui, J. Zhai, L. Cui, S. K. Hutchison, J. F. Simons,

M. Egholm, J. S. Pettis and W. I. Lipkin, *Science*, 2007, **318**, 283–287.
9 J. Klee, A. M. Besana, E. Genersch, S. Gisder, A. Nanetti, D. Q. Tam, T. X. Chinh, F. Puerta, J. M. Ruz, P. Kryger, D. Message, F. Hatjina, S. Korpela, I. Fries and R. J. Paxton, *J Invertebr Pathol*, 2007, **96**, 1–10.
10 M. Higes, M. J. Nozal, A. Alvaro, S. D. Desai, A. Meana, R. Martín-Hernández, J. L. Bernal and J. Bernal, *Apidologie*, 2011, **42**, 364–377.
11 N. Arbulo, K. Antùnez, S. Salvarrey, E. Santos, B. Branchiccela, R. Martín-Hernández, M. Higes and C. Invernizzi, *J Invertebr Pathol*, 2015, **130**, 165–168.
12 J. D. Evans and R. S. Schwarz, *Trends Microbiol*, 2011, **19**, 614–620.
13 D. vanEnglesdorp, J. D. Evans, C. Saegerman, C. Mullin, E. Haubruge, B. K. Nguyen, M. Frazier, J. Frazier, D. Cox-Foster, Y. Chen, R. Underwood, D. R. Tarpy and J. S. Pettis, *PLoS ONE*, 2009, **4**, e6481.
14 E. Genersch, *Appl Microbiol Biotechnol*, 2010, **87**, 87–97.
15 H. L. Holt and C. M. Grozinger, *Journal of Economic Entomology*, 2016, **109**, 1487–1503.
16 W.-F. Huang, L. F. Solter, P. M. Yau and B. S. Imai, *PLoS Pathog*, 2013, **9**, e1003185.
17 J. P. van den Heever, T. S. Thompson, J. M. Curtis, A. Ibrahim and S. F. Pernal, *J. Agric. Food Chem.*, 2014, **62**, 2728–2737.
18 I. Fries, M.-P. Chauzat, Y. P. Chen, V. Doublet, E. Genersch, S. Gisder, M. Higes, D. P. McMahon, R. Martín-Hernández, M. Natsopoulou, R. J. Paxton, G. Tanner, T. C. Webster and G. R. Williams, *Journal of Apicultural Research.*, 2013, **52**.
19 G. E. Cantwell, *Am Bee J*, 1970, **110**, 222–223.
20 A. L. Bourgeois, T. E. Rinderer, L. D. Beaman and R. G. Danka, *J Invertebr Pathol*, 2010, **103**, 53–58.
21 K. A. Aronstein, T. C. Webster and E. Saldivar, *Journal of Applied Microbiology*, 2012, **114**, 621–625.
22 S. Gisder, N. Moeckel, A. Linde and E. Genersch, *Environmental Microbiology*, 2011, **13**, 404–413.
23 S. Fenoy, C. Rueda, M. Higes, R. Martín-Hernández and C. del Aguila, *Appl Environ Microbiol*, 2009, **75**, 6886–6889.
24 Y. Peng, T. F. Lee-Pullen, K. Heel, A. H. Millar and B. Baer, *Cytometry*, 2013, **85**, 454–462.
25 J. W. Snow, *J Invertebr Pathol*, 2016, **135**, 10–14.
26 H. C. Koydemir, Z. Göröcs, D. Tseng, B. Cortazar, S. Feng, R. Y. L. Chan, J. Burbano, E. McLeod and A. Ozcan, *Lab on a Chip*, 2015, **15**, 1284–1293.
27 M. D. Rose, F. Winston and P. Hieter, *Methods in Yeast Genetics: A Laboratory Course Manual (Plainview, New York*, American Psychological Association, Washington, 1990.
28 M. R. Botts, L. B. Cohen, C. S. Probert, F. Wu and E. R. Troemel, *G3 (Bethesda)*, 2016, **6**, 2707–2716.
29 H. C. Hoch, C. D. Galvani, D. H. Szarowski and J. N. Turner, *Mycologia*, 2005, **97**, 580–588.
30 D. Sammataro and J. A. Yoder, Eds., *Honey Bee Colony Health: Challenges and Sustainable Solutions*, CRC Press, Boca Raton, 2011.
31 A. Meana, R. Martín-Hernández and M. Higes, *Journal of Apicultural Research.*, 2010, **49**, 212–214.
32 M. Higes, R. Martín-Hernández, C. Botías, E. G. Bailón, A. V. González-Porto, S. D. Desai, M. J. Del Nozal, J. L. Bernal, J. J. Jiménez, P. G. Palencia and A. Meana, *Environmental Microbiology*, 2008, **10**, 2659–2669.
33 H.-Q. Zheng, Z.-G. Lin, S. K. Huang, A. Sohr, L. Wu and Y. P. Chen, *Journal of Economic Entomology*, 2014, **107**, 2037–2044.
34 M. D. Smart and W. S. Sheppard, *J Invertebr Pathol*, 2012, **109**, 148–151.
35 C. Botías, R. Martín-Hernández, A. Meana and M. Higes, *Parasitol Res*, 2011, **110**, 2557–2561.
36 D. M. Eiri, G. Suwannapong, M. Endler and J. C. Nieh, *PLoS ONE*, 2015, **10**, e0126330.
37 C. J. Jack, H. M. Lucas, T. C. Webster and R. R. Sagili, *PLoS ONE*, 2016, **11**, e0163522.
38 N. Corradi, *Annu Rev Microbiol*, 2015, **69**, 167–183.
39 S. Erler, S. Lommatzsch and H. M. G. Lattorff, *Parasitol Res*, 2011, **110**, 1403–1410.
40 Y. P. Chen and Z. Y. Huang, *Apidologie*, 2010, **41**, 364–374.
41 J. E. Smith, *Parasitology*, 2009, **136**, 1901–1914.
42 G. D. Stentiford, J. J. Becnel, L. M. weiss, P. J. Keeling, E. S. Didier, B. A. P. Williams, S. Bjornson, M. L. Kent, M. A. Freeman, M. J. F. Brown, E. R. Troemel, K. Roesel, Y. Sokolova, K. F. Snowden and L. Solter, *Trends Parasitol*, 2016, **32**, 336–348.
43 H. Zhu, S. O. Isikman, O. Mudanyali, A. Greenbaum and A. Ozcan, *Lab on a Chip*, 2013, **13**, 51–67.
44 X. Xu, A. Akay, H. Wei, S. Wang, B. Pingguan-Murphy, B.-E. Erlandsson, X. Li, W. Lee, J. Hu, L. Wang and F. Xu, *Proc. IEEE*, 2015, **103**, 236–247.
45 D. Zhang and Q. Liu, *Biosensors and Bioelectronic*, 2016, **75**, 273–284.
46 K. Yang, H. Peretz-Soroka, Y. Liu and F. Lin, *Lab on a Chip*, 2016, **16**, 943–958.
47 D. Xu, X. Huang, J. Guo and X. Ma, *Biosensors and Bioelectronic*, 2018, **110**, 78–88.
48 K. E. McCracken and J. Y. Yoon, *Analytical Methods*, 2016.
49 J. D. Evans, *J Invertebr Pathol*, 2006, **93**, 135–139.
50 L. De Smet, J. Ravoet, J. R. de Miranda, T. Wenseleers, M. Y. Mueller, R. F. A. Moritz and D. C. de Graaf, *PLoS ONE*, 2012, **7**, e47953.
51 H. Zhu, U. Sikora and A. Ozcan, *Analyst*, 2012, **137**, 2541.
52 H. Zhu, O. Yaglidere, T.-W. Su, D. Tseng and A. Ozcan, *Lab on a Chip*, 2011, **11**, 315–322.
53 Q. Wei, H. Qi, W. Luo, D. Tseng, S. J. Ki, Z. Wan, Z. Göröcs, L. A. Bentolila, T.-T. Wu, R. Sun and A. Ozcan, *ACS Nano*, 2013, **7**, 9147–9155.
54 I. I. Bogoch, R. K. D. Ephraim, D. Tseng, H. C. Koydemir, A. Ozcan, J. R. Andrews, J. Tee and E. Duah, *The American journal of tropical medicine and hygiene*, 2017, **96**, 1468–1471.

Nosema ceranae detection using a mobile phone